

Hepatic Perfusion Modeling using DCE-MRI with Sequential Breath Holds

Eric M Bultman¹, Ethan K Brodsky², Debra E Horng², Pablo Irarrázaval³, William R Schelman⁴, Walter F Block^{1,2}, and Scott B Reeder^{1,5}

¹Biomedical Engineering, University of Wisconsin-Madison, Madison, WI, United States, ²Medical Physics, University of Wisconsin-Madison, Madison, WI, United States, ³Electrical Engineering, Pontificia Universidad Católica de Chile, Santiago, Chile, ⁴Medicine, University of Wisconsin-Madison, Madison, WI, United States, ⁵Radiology, University of Wisconsin-Madison, Madison, WI, United States

Target Audience: Basic researchers working on liver perfusion imaging, and clinicians interested in hepatic perfusion quantification.

Purpose: To develop and demonstrate the feasibility of a new formulation for quantitative perfusion modeling in the liver using interrupted DCE-MRI data acquired during multiple sequential breath-holds.

Methods: We developed a dual-input single-compartment perfusion model (1) which utilizes a residue function with two degrees of freedom (Weibull function [2]) to better characterize changes between healthy and diseased liver parenchyma. We employed this method to perform hepatic perfusion modeling in a study of 12 healthy volunteers and 9 patients with clinically confirmed HCC. All subjects underwent hepatic DCE-MRI on a clinical 3.0T scanner (Discovery MR750, GE Healthcare; Waukesha, WI) using a 32-channel torso coil (Neocoil; Pewaukee, WI). Data were acquired continuously for 180s using a 3D radial SPGR sequence (3,4) and reconstructed with 4s temporal footprint. Scan parameters included: TR=2.7ms, TE_{1,2,3}=0.4/1.0/1.7ms, flip angle=12°, bandwidth=±250kHz, FOV = 48cm spherical with 256³ matrix and a readout length of 224 points for 2.1mm isotropic spatial resolution.

Subjects were instructed to conduct a 10s pre-contrast breath-hold (BH) at mid-expiration, followed by IV injection of gadobenate dimeglumine (0.1mmol/kg at 2.0mL/s) and 30mL saline chaser at the same rate. Subjects were subsequently instructed to perform three 20-25s BHs during arterial, portal-venous and delayed phases of hepatic enhancement. BHs were coordinated with contrast arrival in the right heart using a real-time display on the scanner console. Average image volumes corresponding to post-injection BHs were rigidly registered to the pre-contrast BH average using a mutual information metric to correct S-I translations between BHs (5). The AIF was determined directly from aortic time-signal data as the aorta is retroperitoneal. The PVIF was determined using the average time-signal curve of a coronal PV ROI (1cm thick) during motion-free BH periods. Motion-corrupted segments of PVIF corresponding to free-breathing were interpolated to generate a continuous PVIF, which is required for convolution.

Perfusion modeling was performed using the AIF and interpolated PVIF as well as average time-signal curves from 1 cm³ ROIs corresponding to normal liver (volunteers), cirrhotic liver (patients), and HCC. These time-signal curves were not interpolated during free-breathing periods. Perfusion maps were generated by fitting time-signal curves of individual voxels using Matlab (lsqcurvefit; Mathworks, Natick MA).

Results: Figure 1 shows the result of fitting average time-signal curves from liver and HCC ROIs to the perfusion model. The HCC ROI demonstrates more rapid and intense enhancement than the liver ROI. Moreover, the HCC ROI closely approximates the enhancement pattern of the aorta, while the liver ROI appears similar to the PVIF – this is consistent with the pathophysiology of HCC, which are known to parasitize blood from the hepatic artery. The fitted time-signal curves (bold lines) are seen to approximate raw data quite well.

Figure 2 shows axial-slice maps of three quantitative perfusion parameters in a patient with multifocal HCC: total perfusion, mean transit time (MTT), and arterial fraction ($k_{art}/(k_{art}+k_{pv})$). Total perfusion is seen to increase in HCC relative to surrounding liver, while MTT is decreased in HCC lesions. The arterial fraction is significantly increased in HCC vs. background cirrhotic liver, consistent with HCC neoangiogenesis.

Discussion: The purpose of this study was to formulate a method for hepatic perfusion modeling using interrupted data from sequential breath-holds, and to test its feasibility. Our results demonstrate that accurate modeling can be performed when data acquired during free-breathing is excluded from model fitting. By excluding motion-corrupted data, quantitative perfusion parameters can be reliably estimated for sub-centimeter focal liver lesions such as small HCC or dysplastic nodules in addition to background liver parenchyma.

Our results also show that quantitative perfusion modeling can distinguish between background cirrhotic liver and HCC. Although identification of HCC can be performed using qualitative DCE-MRI, quantitative perfusion parameters may assist in distinguishing HCC from dysplastic nodules or metastatic disease. Moreover, changes in perfusion parameters which occur shortly after initiation of anti-angiogenic therapy (sorafenib) could be used to assess treatment efficacy (determine responsive patients), which may correlate with long-term survival.

Conclusion: Quantitative perfusion modeling using motion-corrected interrupted DCE-MRI data with PVIF interpolation is feasible.

Acknowledgements: We acknowledge support from the NIH (T32 CA009206, RC1 EB010384, R01 DK083380, R01 DK088925, and R01 DK096169) and the Wisconsin Alumni Research Foundation Accelerator Program. We also wish to thank GE Healthcare for their support.

References: 1. Materne et al, MRM 2001;47:135-42. 2. Cuenod et al, Acad. Radiol. 2002;9:S205-11. 3. Brodsky et al, MRM 2006;56(2):247-54.

4. Brodsky et al, MRM 2012, In Press. 5. Yoo et al, SHTI 2002;85:586-92.

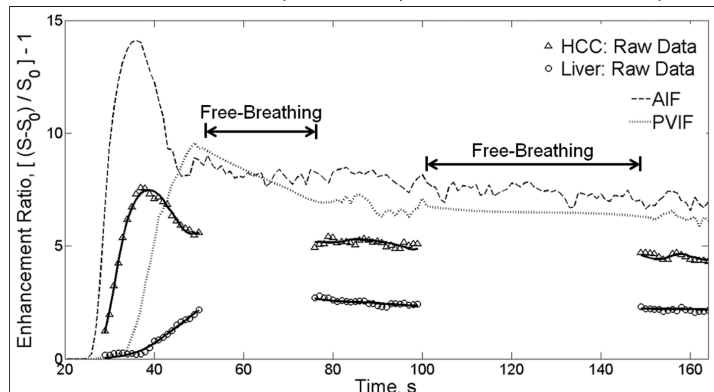


Figure 1: Excellent fitting of the quantitative perfusion model to raw data can be achieved even with gaps in the data during periods of free-breathing. Averaged time-signal curves in a liver ROI (points) and an HCC ROI (triangles) are shown. Fitted curves are overlaid. Note the early arrival of contrast in HCC compared to liver parenchyma, as well as the relationship of these curves to the AIF (dashed line) and PVIF (dotted line). Also note that the PVIF peaks before the end of the arterial phase BH.

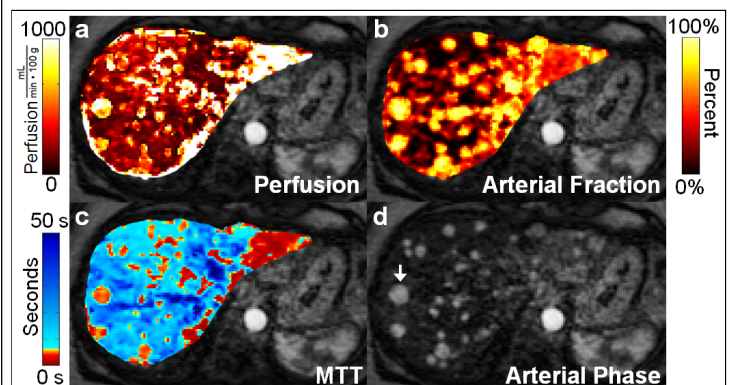


Figure 2: Whole-liver maps of quantitative perfusion parameters depict significant differences between HCC and background hepatic parenchyma. (a) A perfusion map shows increased blood flow to HCC relative to cirrhotic liver (b) An arterial fraction map shows increased arterial perfusion in HCC (c) An MTT map shows decreased transit times of contrast through HCC lesions (d) An arterial phase slice shown for reference (white arrow = HCC)